Biochemical and High Throughput Microscopic Assessment of Fat Mass in Caenorhabditis Elegans

Video Article

Biochemical and High Throughput Microscopic Assessment of Fat Mass in *Caenorhabditis Elegans*

Elizabeth C. Pino[1], Christopher M. Webster[1], Christopher E. Carr[2], Alexander A. Soukas[1]

[1]Center for Human Genetic Research and Department of Medicine, Massachusetts General Hospital and Harvard Medical School

[2]Department of Earth, Atmospheric, and Planetary Sciences, Massachusetts Institute of Technology

Correspondence to: Alexander A. Soukas at asoukas@chgr.mgh.harvard.edu

URL: http://www.jove.com/video/50180
DOI: doi:10.3791/50180

Keywords: Genetics, Issue 73, Biochemistry, Cellular Biology, Molecular Biology, Developmental Biology, Physiology, Anatomy, Caenorhabditis elegans, Obesity, Energy Metabolism, Lipid Metabolism, C. elegans, fluorescent lipid staining, lipids, Nile red, fat, high throughput screening, obesity, gas chromatography, mass spectrometry, GC/MS, animal model

Date Published: 3/30/2013

Citation: Pino, E.C., Webster, C.M., Carr, C.E., Soukas, A.A. Biochemical and High Throughput Microscopic Assessment of Fat Mass in *Caenorhabditis Elegans*. *J. Vis. Exp.* (73), e50180, doi:10.3791/50180 (2013).

Abstract

The nematode *C. elegans* has emerged as an important model for the study of conserved genetic pathways regulating fat metabolism as it relates to human obesity and its associated pathologies. Several previous methodologies developed for the visualization of *C. elegans* triglyceride-rich fat stores have proven to be erroneous, highlighting cellular compartments other than lipid droplets. Other methods require specialized equipment, are time-consuming, or yield inconsistent results. We introduce a rapid, reproducible, fixative-based Nile red staining method for the accurate and rapid detection of neutral lipid droplets in *C. elegans*. A short fixation step in 40% isopropanol makes animals completely permeable to Nile red, which is then used to stain animals. Spectral properties of this lipophilic dye allow it to strongly and selectively fluoresce in the yellow-green spectrum only when in a lipid-rich environment, but not in more polar environments. Thus, lipid droplets can be visualized on a fluorescent microscope equipped with simple GFP imaging capability after only a brief Nile red staining step in isopropanol. The speed, affordability, and reproducibility of this protocol make it ideally suited for high throughput screens. We also demonstrate a paired method for the biochemical determination of triglycerides and phospholipids using gas chromatography mass-spectrometry. This more rigorous protocol should be used as confirmation of results obtained from the Nile red microscopic lipid determination. We anticipate that these techniques will become new standards in the field of *C. elegans* metabolic research.

Video Link

The video component of this article can be found at http://www.jove.com/video/50180/

Introduction

Conservation of metabolic pathways between humans and the nematode *Caenorhabditis elegans* makes it a powerful model organism for the study of obesity. While *C. elegans* do not have adipocytes dedicated to fat storage like in mammals, they do store triglycerides in lipid droplets[1] and possess many of the same regulators of fat storage and energy use[2,3]. To assay for fat levels in *C. elegans*, several methods have been proposed with varying levels of ease and success. The once common use of fluorescent, vital dyes[4-7] was recently called into question, and these reagents proved to be staining a compartment distinct from the main fat storage depot of *C. elegans*[1,8-11] . Fixative-based non-fluorescent dyes, such as Sudan black and Oil-red-O, while successful at highlighting lipid droplets in the worm[12-14], do not have as large a dynamic range for quantitation as fluorescent dyes[8,13,15]. Furthermore, current methods of fixation for both fluorescent and non-fluorescent dyes are time-consuming and involve multiple freeze-thaw steps and/or the use of toxic chemicals[1,9,10] . The use of specific BODIPY-labeled lipid analogs has been reported to highlight lipid droplets when fed to living worms with short-term labeling[15]. However this relies on uptake of the dye and is therefore biased by *C. elegans* handling and metabolism of BODIPY fatty acid analogs. An established alternative to lipid-staining dyes is label-free, coherent anti-Stokes Raman scattering (CARS) or stimulated Raman scattering (SRS) microscopy, which take advantage of the characteristic vibrational properties of lipid molecules to visualize fat stores[10,16,17] . However, expensive specialized equipment is necessary for this method, and throughput is low at best.

To fulfill a need for rapid, scalable analysis of neutral lipid stores in *C. elegans* metabolic research, we introduce a novel, highly reproducible method of fixative-based Nile red lipid staining. Spectral and physicochemical properties of the lipophilic dye Nile red induce a yellow-gold-spectral shift in its excitation-emission peak, allowing it to fluoresce in the green emission spectrum only when in a lipid-rich environment, but not in more polar environments[18,19] . Thus lipid droplets can be detected after simple staining by the use of a green fluorescent protein (GFP) filter set for fluorescence microscopy. The ease and affordability of this technique make it ideally suited for high throughput screens. We also demonstrate a paired, rigorous method for biochemical determination of triglycerides and phospholipids using solid phase extraction and gas

chromatography-mass spectrometry. Biochemical lipid measurement correlates with Nile red-based microscopic determination of *C. elegans* fat mass, and should be used as a confirmation of findings made with microscopic lipid determination.

Protocol

1. Preparation of Rectangular Amp/Tet (A/T) LB Agar Plates and NGM IPTG RNAi Plates

A/T plates should be prepared 1-4 weeks prior to use and stored in the dark at 4 °C.

1. For 1 L of media add 1 L deionized water, 32 g LB agar, 1.5 ml 2 M NaOH, and 2 g Bacto agar. Autoclave 40 min on liquid cycle. After cooling to 60 °C, add 3 ml tetracycline and 0.5 ml ampicillin. Pour 45 ml of media into each plate.

Prepare 96-well RNAi plates 3 days up to 2 weeks in advance.

2. To pour 25 96-well RNAi plates, prepare 1 L of nematode growth media (NGM): 1 L deionized water, 3 g NaCl, 17 g agarose, and 2.5 g bactopeptone. Autoclave liquid cycle at 121 °C for 40 min with a stir bar. Let cool, stirring on a hot plate set to 60 °C.
3. When cool to 60 °C, add the following stock solutions: 1 ml 1 M $MgSO_4$, 1 ml 5 mg/ml cholesterol, 25 ml 1 M KH_2PO_4 (pH 6.0), 1 ml 1 M $CaCl_2$, 1 ml 200 mg/ml carbenicillin, and 5 ml 1 M IPTG (see Materials table for recipes).
4. Dispense 150 µl of RNAi media into each well of a flat-bottomed 96-well plate using an electronic multichannel pipettor. Avoid air bubbles. Keep media in a sterile stainless steel receptacle immersed in a 60 °C water bath while dispensing.
5. Keep RNAi plates level until agarose solidifies. Plates can be poured up to 2 weeks in advance and stored at 4 °C.

Day 1

2. Stamp Frozen Library Plates onto Rectangular Amp/Tet (A/T) LB Agar Plates

1. Warm A/T plates to room temperature, keeping them in the dark.
2. Transfer 96-well RNAi library plates from -80 °C to dry ice. Open the aluminum-sealed plate near a Bunsen burner.
3. Sterilize a 96-pin replicator by immersing pins serially (10 sec each) in 10% bleach, deionized H_2O, and 70% EtOH followed by passing pins through a flame. Repeat EtOH and flame step.
4. Apply replicator to frozen 96-well RNAi glycerol stock, making sure each pin contacts the surface of each well.
5. Stamp onto A/T plate, drawing a small circle with each pin without damaging agar surface.
6. Re-seal and return library plates to -80 °C. Incubate stamped A/T plates at 37 °C overnight for bacterial growth.

Day 2

3. Grow RNAi Bacterial Clones Overnight in Deep-well Blocks

1. Remove A/T plates from 37 °C and confirm bacterial growth.
2. Fill each well of a 96-well deep-well block with 1.5 ml of LB with 200 µg/ml carbenicillin.
3. Sterilize 96-pin replicator (see step 2.3).
4. Apply replicator to the top of the A/T plate, making sure pins make contact with each bacterial RNAi clone. Lift replicator and immerse pins into the deep-well block. Swirl, and slowly remove, making certain not to contaminate adjacent wells.
5. Seal block with breathe-easy film. Incubate overnight at 37 °C with agitation (950 rpm in MT Infors Microtiteron II shaker, preferred, or 250 rpm in a 25 mm-throw shaking incubator).

Day 3

4. Seed RNAi Bacterial Clones onto 96-well NGM RNAi Plates

1. Remove 96-well RNAi plates from 4 °C and warm to room temperature.
2. Remove deep-well blocks and centrifuge 10 min at 4,000 x g.
3. Rapidly invert blocks into sink to drain media, and stamp inverted onto paper towel to eliminate excess media.
4. Under a laminar flow hood, add 40 µl of LB with 200 µg/ml carbenicillin to each well and seal with sterile film.
5. Return blocks to room temperature bacterial shaker for 10 min to resuspend pellets, or manually resuspend pellets by careful pipetting.
6. In the laminar flow hood, remove sterile film and transfer bacteria from deep-well blocks onto 96-well RNAi plates. Add 40 µl of resuspended bacteria to rows 'A' and 'H', and 35 µl from all other rows. More liquid is added to edge wells of the 96-well RNAi plate to prevent overdrying and cracking of the agarose.
7. Leave plates uncovered to dry in hood for 4-6 hr, inspecting regularly for dryness. Dry bacteria appear clear, not cloudy. Cover, invert plates and incubate at room temperature overnight.

5. Prepare a Synchronous Population of Worms

Two 10 cm plates filled with many gravid worms are used for egg preparation for every 6 96-well RNAi plates. Be sure worms are non-starved for at least two generations (7 days).

1. Prepare a synchronous population of L1 as previously described[20]. For 20 ml of bleach solution, use 4 ml bleach, 1 ml NaOH (10 M), 5 ml deionized H_2O, and 10 ml M9 buffer.
2. Synchronize worms overnight in 10 ml M9 in a 15 ml sterile polypropylene tube with rotation at 20 °C.

Day 4

6. Add Worms to RNAi Plates

1. Centrifuge egg preps at 3,000 x g for 1 min. Aspirate supernatant, staying away from the pellet of L1 hatchlings. Resuspend in 5 ml M9 buffer with 0.0005% Triton X-100. Addition of the small amount of detergent prevents worms from sticking to the pipette and has no effect on fat staining.
2. Count worms under a microscope. If necessary, adjust concentration to 10-15 worms per microliter.
3. In the laminar flow hood, for each 96-well plate to be seeded, add 75 µl of resuspended worms into each well of one row of a shallow-well assay block. Using a manual multichannel pipette, add 50-75 worms in 5 µl into each well of the 96-well RNAi plates.
4. Allow plates to dry in the hood for 30 to 60 min. When dry, under a microscope, worms should appear to be crawling, not thrashing.
5. Grow worms on RNAi plates at 20 °C for ~64 hr.

Day 7

7. Fix and Stain Worms in Nile Red

1. Remove RNAi plates from incubator. Examine under microscope and record starved or thrashing (wet) wells to exclude from further analysis, as these conditions affect fat mass.
2. Using an electronic repeat pipettor, add 150 µl PBS with 0.01% triton X-100 to each well of an RNAi plate. With a manual multi-channel pipettor, mix and transfer liquid with worms to the corresponding row in a 96-deep-well PCR plate. Avoid disrupting the agar. Repeat for a total of 300 µl worms in PBS per well.
3. When four plates have been transferred, centrifuge plates at 500 rpm for 1 min.
4. Aspirate supernatant using a 96-pin vacuum aspirator, leaving ~25 µl liquid and worm pellet at the bottom of the well.
5. Add 150 µl of 40% isopropanol to each well to fix animals. Make certain that pipettor is on a high enough speed to mix worm pellet with 40% isopropanol. Incubate at room temperature for 3 min.
6. Centrifuge plates uncovered at 500 rpm for 1 min.
7. Aspirate supernatant using a 96-pin aspirator or manually, leaving only 25 µl 40% isopropanol + worm pellet at the bottom of the well.
8. To each well, add 150 µl of Nile red staining solution prepared immediately before use: 6 µl Nile red stock solution of 0.5 mg/ml in acetone per 1 ml of 40% isopropanol.
9. Seal plate with non-sterile adhesive film and stain in the dark for at least 2 hr.

8. Wash and Image Worms on a High-throughput Microscope

1. Centrifuge at 500 rpm for 1 min and aspirate all but 25 µl of Nile red dye.
2. Add 150 µl of PBS with 0.01% triton X-100 to each well and store in the dark for at least 30 min.
3. Centrifuge at 500 rpm for 1 min.
4. Using a 12-channel pipettor, aspirate animals from the bottom of each well with 2 x 7 µl quick strokes and dispense onto a 96-well Teflon-printed glass slide. Carefully, without removing worms, remove 9.5 µl of PBS from each well of slide. If your glass slide does not fit directly in your microscope mount, a custom machined aluminum slide holder must be used to mount worms.
5. Slowly lower cover slide onto 96-well slide. This step may take some practice to avoid bubbles or cross over of worms into other wells. Secure corners with adhesive tack.
6. Image slide in bright field and fluorescence with a GFP/FITC filter set on an automated microscope. The lipid signal photobleaches easily so it should be imaged in a systematic way in all wells, not manually, as photobleaching will lead to artificial differences between wells. For more details on analysis, please see Representative Results and Discussion.

9. Biochemical Lipid Determination Using Solid Phase Extraction (SPE) and Gas Chromatography-Mass Spectrometry (GC/MS)

For validation of lipid levels based on Nile red fluorescence, gas chromatography followed by mass spectrometry analysis (GC/MS) can be performed on fatty acid methyl esters (FAME) derived from triacylglycerols (TAG) and phospholipids (PL) from worm pellets. Steps involving organics should be performed under a fume hood. Care should be taken that lipids are kept under nitrogen protected from light during extended storage or incubation steps as they are very vulnerable to oxidation. Worm pellets from 2,500-5,000 synchronous animals are used as input, prepared exactly as above except that animals are grown on 10 cm RNAi plates.

1. Wash 2,500-5,000 worms from each 10 cm plate with 10 ml M9 buffer into a 15 ml conical polypropylene tube. Pellet worms at 500 x g for one minute, and wash pellet again with 10 ml M9 buffer. Pellet animals at 500 x g. Aspirate leaving 250 µl total volume, and either freeze on liquid nitrogen and store at -80 °C under nitrogen for later processing or proceed directly.
2. The worm pellet may be taken directly to step 9.3 if triglyceride mass is to be normalized to phospholipid mass[8,13,21] . However, if the investigator desires normalization to protein content or DNA content, the worm pellet should be sonicated on the highest intensity in a bath sonicator for 10 min, 30 sec on, 30 sec off, at 4 °C. If protein or DNA normalization is desired, remove a 5 µl aliquot and determine total protein concentration using a Bradford reagent or similar or total DNA content after column purification using a UV spectrophotometer.

3. Add worms to 1.5 ml 2:1 chloroform:methanol in a threaded borosilicate glass tube. All transfer of organic solvents should be done using glass pipettes.
4. Using a wiretrol 50 µl pipette, add 25 nM phospholipid standard in 50 µl, and 16.7 nM triglyceride standard in 50 µl. Both standards should be dissolved in 2:1 chloroform:methanol, capped tightly, and stored under nitrogen protected from light in a -80 °C freezer to avoid oxidation.
5. Cap with phenolic cap and vortex. Extract for 1 hr at RT, vortexing every 15 min.
6. Centrifuge at 1,000 rpm for 5 min. Transfer lower organic phase without carcasses to a borosilicate culture tube.
7. Add 0.3 ml 0.9% NaCl, vortex and centrifuge at 1,000 rpm for 5 min.
8. Transfer bottom organic layer to a fresh borosilicate culture tube, making sure not to transfer over any of the aqueous phase.
9. Dry organic phase under nitrogen. To begin solid phase extraction (SPE) resuspend dried lipid in 1 ml chloroform. Alternatively, for detailed separation and analysis of distinct lipid classes, including phospholipid classes, glycolipids, sphingolipids, diacylglycerols, triacylglycerols, free fatty acids, and cholesterol esters, thin layer chromatography as pioneered by the Watts lab in *C. elegans*[22] may be used in place of SPE. Lipids may also be separated by HPLC and fractions analyzed by GCMS . Sophisticated methods of whole-lipidome profiling by liquid-chromatography/MS (LCMS) can also be used[23-26].
10. Assemble silica SPE column on SPE manifold. Pre-equilibrate column with 3 ml chloroform. Allow solvent to flow by gravity.
11. Load lipid sample onto SPE column, collecting flow-through in a threaded borosilicate tube as part of the first fraction (TAG fraction). Most neutral lipids will come through in this first 1 ml flow-through. Add 3 ml chloroform to fully elute TAG fraction, collecting flow-through in the TAG fraction tube.
12. Remove and cap the first collection tube, and replace with a clean collection tube. Elute glycosphingolipids with 5 ml of 9:1 acetone:methanol. We do not routinely analyze the fatty acid composition of this fraction, however, it may contain valuable information and can be saved for preparation of methyl esters and free sphingoid bases for further analysis utilizing specialized procedures distinct from those for TAG and PL as previously described [27].
13. Replace glycosphingolipid collection tube with a second threaded borosilicate collection tube. Elute phospholipids with 3 ml methanol (PL fraction).
14. Fractions can be stored at -80 °C at this point capped tightly under nitrogen. Dry purified lipids under nitrogen. To speed drying, in a dry heating block at 33 °C. Never store lipids in dried form, as they are especially susceptible to oxidation in the dried state.
15. Resuspend dried lipid fractions in 2 ml 2% H_2SO_4 in methanol by vortexing and incubate capped tightly overnight in a 55 °C water bath to create FAMEs. Care must be taken to get absolutely no water in the FAME reaction as this will greatly inhibit derivatization of lipids. We have found more efficient derivatization by overnight incubation and the literature suggests less lipid oxidation occurs at lower temperatures during FAME preparation[28]. An alternate and more rapid method is to use 2 ml 2.5% H_2SO_4 in methanol and derivatize for one hour at 70 or 80 °C[21,22,29] .
16. The next morning, remove from bath, and allow to cool. Add 1.5 ml H_2O (to quench the reaction) and then 0.3 ml hexane (to extract the FAMEs) to each TAG and PL fraction. Shake vigorously and centrifuge at 1,000 rpm for 5 min.
17. Very carefully remove only top hexane layer using a standard pipette or Pasteur pipette. Dispense into autosampler tube. Make certain not to include any acidified methanol as this will destroy the GC column and MSD.
18. Cap and load samples onto GC/MS. The sample is transferred in hexane to a micro-insert Agilent vial capped with a PTFE-silicone-PTFE screw cap. It is transferred to the Agilent GCMS model 6890/5973N outfitted with a Supelcowax-10 (24079) 30 meter, 250 micron fused silica capillary column. One microliter is injected into a splitless inlet set at 250 °C and 13.33 P.S.I. Ultrapure Helium is used a carrier gas. The protocol run is as follows at a constant 1 ml per min:

Step	Instruction	Goal Temperature
1	Hold 2 min	150 °C
2	Ramp 10 °C per min	200 °C
3	Hold 4 min	200 °C
4	Ramp 5 °C per min	240 °C
5	Hold 3 min	240 °C
6	Ramp 10 °C per min	270 °C
7	Hold 5 min	270 °C

A 3 min solvent delay is used at the MSD to minimize wear on the filament. Thereafter, masses between 50 and 550 Daltons are detected with the MS quadruple set at 150 °C and the ms source set at 230 °C, with a thermal auxiliary temperature of 270 °C.

Representative Results

An example of an imaged plate that has been taken through the fat staining workflow is shown in **Figure 1**. Specific controls for high fat (*daf-2* insulin receptor RNAi), low fat (*lpd-3* protein required for lipid storage granules in the gut RNAi), small and low fat (*fasn-1* fatty acid synthase RNAi), and empty vector (control) show the variations in fluorescence intensity according to the fat levels of the animals, and the corresponding lipid amounts determined by GC/MS analysis (**Figure 2**). Note that gene inactivations leading to developmentally arrested, small animals will often appear to have much lower fat than adult control animals, irrespective of any connection to fat metabolism (**Figure 3**). Secondary analyses, including staining analysis and lipid biochemistry with SPE-GCMS of wild-type control animals of a similar developmental stage must be done to ensure the validity of small or developmentally arrested positive hits. In the case of *fasn-1* RNAi (**Figure 2**), animals arrest in either the L2 or L3 larval stage, and have fat staining lower than adult control RNAi, but similar in abundance to L2-L3 stage control RNAi animals (fat stain percent of adult control RNAi: 49.9 ± 4.5% for *fasn-1* RNAi and 20.2 ± 2.1% for L2 control RNAi, and 64.7 ± 1.3 for L3 control RNAi). Alternatively, biochemical analysis indicated a lower TAG/PL ratio than L2 stage matched N2 control animals (TAG/PL: 22.5 ± 2.9 for *fasn-1* RNAi and 46.1

± 3.4 for stage-matched control RNAi, $P \leq 0.05$). Thus in this instance it can be confirmed by biochemical analysis that fasn-1 has a role in lipid storage rather than just a stage-specific reduction in fat mass.

The follow-up analysis of imaged worms relies heavily on a computational platform such as Cell Profiler using the WormToolbox[30]. For smaller numbers of images, a publicly available image analysis platform such as ImageJ, freely available from the NIH, may be used. For our analysis, unique Matlab scripts were used first to identify the well, and subsequently to exclude empty wells or those with bubbles, and distinguish small debris from worms. Manual quality control was necessary for images flagged for exclusion for the reasons mentioned above. We found empirically that 90th percentile intensity of worm pixels across a well, normalized to worm area across a well, provided consistent metric of staining intensity at all stages of worm development (**Figure 3**). Integrating total fat mass over the area of the worm, on the contrary, would tend to score small bright worms equivalently with large dim worms. Because our method does not integrate total fluorescent signal over the area of the worm, in taking an intensity percentile, changes in worm size per se do not bias the intensity measured. Instead, differences in the pixel intensity distribution are measured. However, in spite of this, pronounced differences are seen in staining pixel intensity distribution between animals of different developmental stages, so it is important to study the effect of RNAi to any gene against animals of a comparable developmental stage (**Figure 3**). Average variability between replicates is shown in **Figure 4** indicating high reproducibility of the fat staining method. Note that the strength of the method is highly dependent on obtaining quality images for each plate, under uniform illumination conditions, using identical exposure times, and with minimal bubbles, debris, or crossover of worms into other wells.

SPE was performed on pre-mixed, purified standards to determine the degree to which TAGs could be separated from PLs (**Figure 5A**). In this analysis, we achieved a 100% separation of TAG and PL, indicated as a complete absence of 17:0 fatty acids derived from PL in the TAG sample and a corresponding complete absence of 13:0 fatty acids derived from TAG in the PL sample (**Figure 5A**). Thus SPE is highly efficient at separating lipid classes. This analysis does not indicate that all TAGs of different chain lengths will be purified equivalently by SPE and detected by GCMS with similar efficiency. It only assures that TAG and PL lipids in total are completely separated from each other.

A sample GC-MS trace of N2 wild type animals taken through solid phase extraction and FAME preparation is shown in **Figure 5B**. For both TAG and PL, peaks can be identified based upon retention time and parent and daughter ions on the mass spectrum, and the total area under the identified peaks normalized to the area of the respective internal standards. To determine the normalized amount of TAG, the area under all peaks of the TAG chromatogram, except the 13:0 standard, were added together and divided by the area under the 13:0 peak. Likewise, to determine the normalized total PL amount, the area under all peaks, except the 17:0 standard, were added together and divided by the area under the 17:0 peak. The normalized values for the TAG and PL samples are then used to calculate the final TAG/PL ratio for the sample:

$$\text{TAG:PL Ratio} = \frac{\frac{\Sigma Area(TAG\ All\ Peaks\ except\ 13{:}0)}{Area(13{:}0)}}{\frac{\Sigma Area(PL\ All\ Peaks\ except\ 17{:}0)}{Area(PL\ 17{:}0)}}$$

It should be noted that the data from SPE-GCMS permit a much more sophisticated analysis of fatty acids present in each lipid fraction than simple calculation of the total TAG to PL ratio. For example, the investigator can integrate a single peak corresponding to a single fatty acid and compare its normalized abundance across samples (*e.g.* comparing in N2 wild-type versus *daf-2* RNAi the integrated area of the 18:0 peak divided by the 13:0 standard peak, normalized to total PL mass divided by PL 17:0 standard peak area):

$$\text{Relative Abundance 18:0} = \frac{\frac{Area(N2\ TAG\ 18{:}0)}{Area(N2\ TAG\ 13{:}0)}}{\frac{\Sigma Area(N2\ PL\ All\ Peaks\ except\ 17{:}0)}{Area(N2\ PL\ 17{:}0)}} \Big/ \frac{\frac{Area(daf{-}2\ RNAi\ TAG\ 18{:}0)}{Area(daf{-}2\ RNAi\ TAG\ 13{:}0)}}{\frac{\Sigma Area(daf{-}2\ RNAi\ PL\ All\ Peaks\ except\ 17{:}0)}{Area(daf{-}2\ RNAi\ PL\ 17{:}0)}}$$

Should the investigator choose, it would also be possible to determine the percentage of any given fatty acid in the TAG or PL fractions as a percentage of the total amount of fatty acid quantitated (as an example 18:0 in the TAG fraction in N2 worms):

$$\text{Percent Abundance 18:0} = \frac{Area(N2\ TAG\ 18{:}0)}{\Sigma Area(N2\ TAG\ All\ Peaks\ except\ 13{:}0)} * 100$$

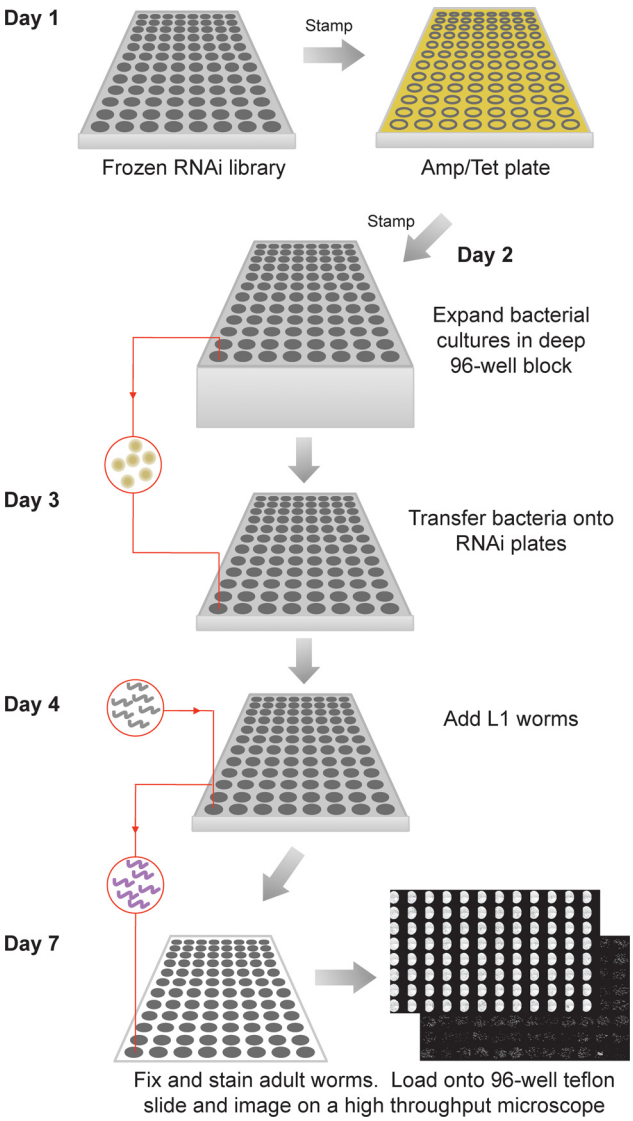

Figure 1. Typical workflow for the overall experiment. Day 1, frozen RNAi library plates are stamped onto Amp/Tet LB agar plates and incubated at 37 °C. Day 2, Amp/Tet plates are used to seed liquid cultures of RNAi clones in deep well blocks. Day 3, bacteria are concentrated by centrifugation and transferred to 96-well RNAi plates. Day 4, L1 hatchling *C. elegans* are added to RNAi plates in liquid and allowed to dry. Day 7, animals are collected in liquid, stained with Nile red in 40% isopropanol, mounted on 96-well Teflon slides, and imaged with a high-throughput microscope.

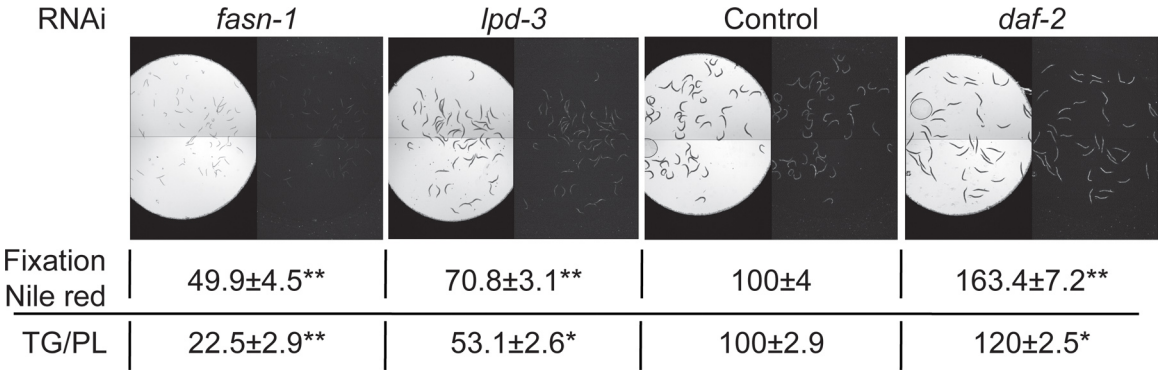

Figure 2. Fixative-based Nile red stains major *C. elegans* fat stores. Representative bright field and GFP fluorescence images are shown of N2 worms fed on *fasn-1* (small, low fat), *lpd-3* (low fat), control (empty vector), or *daf-2* (high fat) RNAi clones. Samples were processed as per the protocol (schematic in **Figure 1**). Animals fixed, stained in Nile red, and imaged result in comparable lipid levels as obtained from biochemical lipid measurement. Isopropanol-fixed Nile red fluorescence levels, acquired from at least 6 biological replicates, are shown in the first row. Quantitative triglyceride levels, reflective of overall neutral lipid stores when normalized to overall phospholipid levels (TAG/PL), taken from 4 biological replicates, are shown in the second row. It is important to note that the absolute quantitation achieved from fixative Nile red staining and biochemical lipid determination often do not match perfectly. In this instance, though qualitatively similar, *fasn-1*(RNAi) has more different triglyceride mass vs. control by biochemical methods than indicated by microscopy, *lpd-3* is comparably different, and *daf-2*(RNAi) is less different, though all differences are highly statistically significant and measurements were highly reproducible. Data shown are mean ± SEM (*, $P \leq 0.01$; **, $P \leq 0.0001$ relative to control, determined by unpaired, two-tailed T-test assuming equal variance).

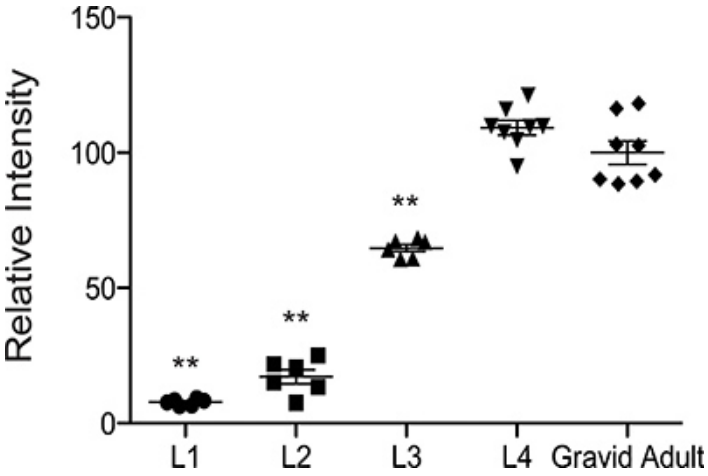

Figure 3. Fat mass determined by fixation Nile red staining at different larval stages. Animals were grown on OP50 bacteria and collected at the L1, L2, L3, L4 and gravid adult developmental stages. Images were captured following fixation staining and analyzed using a customized Matlab script to determine the 90th percentile of pixel intensity over the identified worm area. Note that the lipid levels of animals greatly increase as the animal develops from L2 to L4 stage, and then decrease slightly as the animal begins to divert calories toward the proliferation of the germline in the adult stage. Data shown are mean ± SEM for 6-8 replicates (**, $P \leq 0.0001$ relative to gravid adult, determined by unpaired, two-tailed T-test).

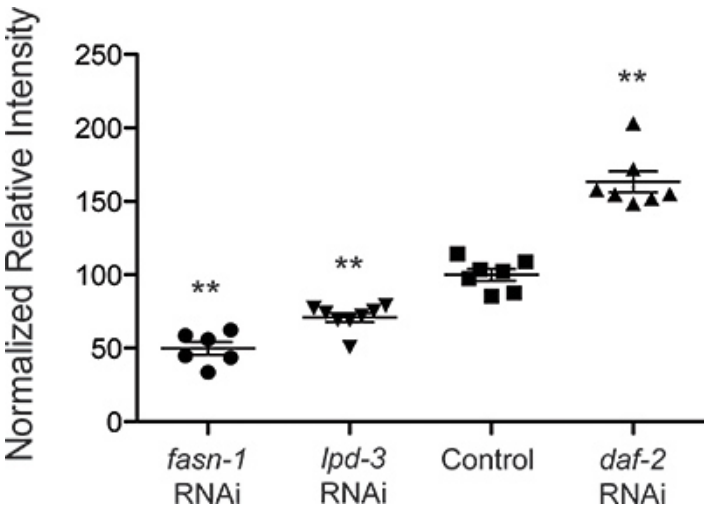

Figure 4. High reproducibility across independent biological replicates. Shown is a scatter plot of Nile red fluorescence intensities across biological replicates (n = 6-8). For each replicate, all values are normalized to the mean intensity of the empty vector controls. Data shown are mean ± SEM (**, $P \leq 0.0001$ relative to control, determined by unpaired, two-tailed T-test assuming equal variance).

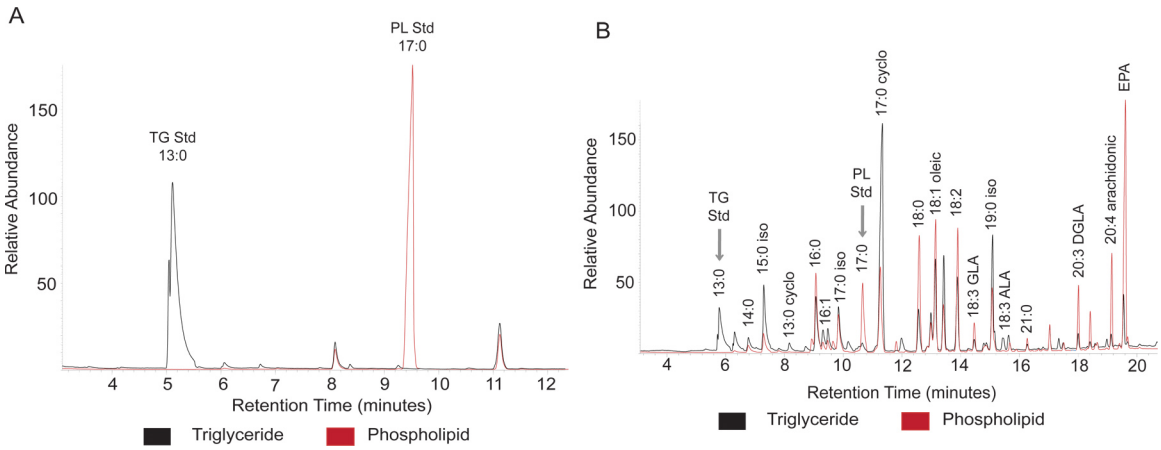

Figure 5. GC-MS chromatograms of SPE separated standards and wild type TAG and PL abundance. (A) GC-MS traces are shown of the SPE separation of TAG and PL standards. Note the complete absence of 13:0 fatty acid in the PL trace and the corresponding absence of the 17:0 fatty acid in the TAG trace, indicating complete separation of TAG (tritridecanoin) from PL (1,2-diheptadecanoyl-*sn*-glycero-3-phospho-(1'-*rac*-glycerol)). (B) A representative full spectrum of TAG and PL from a sample of N2 wild type animals fed vector control RNAi (HT115 bacteria with L4440 empty vector RNAi). One microliter of sample was injected into an Agilent 6890/5973N GCMS according to the protocol, and individual peaks were identified by retention time and their respective mass spectra. Abbreviations: cyclo, cyclopropane fatty acid; iso: iso-methyl branched chain fatty acid; GLA, gamma linolenic acid; ALA, alpha linolenic acid; DGLA, dihomo gamma linolenic acid; EPA, eicosapentaenoic acid. Click here to view larger figure.

Discussion

The presented protocol allows for rapid, large scale screening of lipid levels in *C. elegans*, which can be easily adapted to high throughput screens. Unlike previously used methods, which involve a lengthy fixation step in paraformaldehyde followed by several freeze-thaw cycles[8,10], our protocol requires a simple 3-min fixation in isopropanol. We have found that by staining *C. elegans* in 40% isopropanol, they become freely permeable to Nile red, without the use of additional freeze-thaw or fixation steps. Also, as Nile red selectively fluoresces in hydrophobic compartments in the green spectrum[18,19,31], no destaining is necessary. In total, animals can be taken from RNAi plates to stained and ready to image animals in just over 2.5 hr. This method can be performed relatively inexpensively and with high reproducibility. The method does not depend upon the ability of *C. elegans* to uptake or concentrate the dye, and therefore does not have the same limitations as feeding based methods using vital dyes. Given reproducibility and precision of measurements, the method is suitable for screening large numbers of gene inactivations by RNAi. If quantitation of lipid levels is desired based upon fixative Nile red staining, we recommend the use of 4-6 biological replicates with the appropriate controls and statistical testing applied.

It is likely that many gene inactivations leading to small animals (due to RNAi clones causing delayed or arrested development) would come out of a screen for fat regulators, regardless of any connection to fat metabolism. While the image analysis program we utilized accounts for worms of different sizes by normalizing the fluorescence intensity to the worm area, individual researchers may also want to consider

comparing the fat staining levels of small animals to wild type animals of a similar developmental stage. In the case of small or developmentally arrested animals with apparent low fat mass, we suggest that no single modality is sufficient to demonstrate altered lipid metabolism. Several follow-up experiments, including SPE-GCMS, could be required to ascertain the lipid-regulatory function of these genes. For known metabolic regulator *fasn-1*, SPE-GCMS analysis compared to developmentally matched N2 L2 control animals was necessary to confirm the apparent low fat phenotype found when compared to adult control animals. While Nile red fat staining indicated lower fat levels relative to control adult RNAi, when compared to stage-matched L2 control RNAi animals, no apparent difference was seen. Accordingly, use of a second method, *i.e.* biochemical quantification of the TAG/PL ratio was necessary to determine that *fasn-1* is a true regulator of fat mass, as *fasn-1* RNAi is biochemically distinguishable from stage-matched L2 control RNAi animals.

While we present imaging and processing for a high-throughput platform, a conventional upright microscope can easily be used to capture images from worms mounted on agarose pads[20] or on conventional sized Teflon-printed 8 to 12 well microscope slides. The only limitation is that as the green fluorescence of lipid droplets stained with Nile red photobleaches quickly, systematic, uniform exposure conditions need to be used to ensure comparability between images. We find that a fully automated microscope with uniform image acquisition conditions works best to this effect.

One of the great strengths of this protocol is that after images are collected they may be saved for future re-analysis. The same images could be used to determine body size in addition to fat content. Moreover, as computational programs become more advanced, there is the prospect for single worm analysis, generating statistically significant results from a single well. Thus our method that utilizes high-throughput microscopy has some advantages over published screen methodologies that use a Copas Biosort to quantify fluorescent signals[32,33] . However, the methodologies are definitely complimentary.

Precise, biochemical determination of lipid content by SPE and GC/MS confirms the Nile red staining of the major fat stores in *C. elegans*. Although the absolute quantitation achieved from fixative Nile red staining and biochemical lipid determination often do not match perfectly, both methods produce highly reproducible, statistically significant results that agree qualitatively. In addition, this method can be tailored to meet the specific needs of individual researchers who may require further analysis of the separate classes of glycosphingolipids, phospholipids, or triglycerides present in various samples. It should be noted that other groups have used technology other than SPE to separate lipid classes prior to GC/MS[22]. Thin layer chromatography (TLC) and high pressure liquid chromatography (HPLC) has advantages over SPE in that they might be able to better separate distinct neutral lipids (*e.g.* TAG, diacylglycerols, free fatty acids, and cholesterol esters) from polar lipids (phosphatidylcholine, phosphatidylethanolamine) and glycol-sphingolipids. We choose SPE because it requires a minimum of starting material (2,500-5,000 worms), it emphasizes the major long-term energy stores, TAGs, which make up most of the neutral lipid fraction[4], and is rapid, requiring no specialized equipment or plates. It should be emphasized that based upon standard mixtures, SPE completely separates TAGs from PLs, and is highly reproducible and reliable (see **Figure 5A**). While quantitation and analysis of fatty acid methyl esters requires a GC/MS, this equipment is commonly available, and if not locally, samples may be generated as above and stored at -80 °C under nitrogen until analysis by a collaborator or commercial GC/MS service is arranged.

The GCMS output contains high-resolution data on each fatty acid within each lipid species. This permits the determination of detailed differences between samples compared. As an example, the investigator could determine whether the levels of certain fatty acids were altered in abundance more significantly than others in *daf-2*, *lpd-3* or *fasn-1* RNAi versus vector control. This enormously powerful tool can therefore provide detailed information on which lipid species are altered in abundance with any experimental manipulation.

For our analysis, we most often normalize TAG mass to PL mass. While protein or DNA could also be used to normalize lipid mass following determination from an aliquot of sonicated worm pellet, we find that these methods are subject to introduced human error during all pipetting steps and in sample recovery from each extraction. It is for this reason that we chose to instead use PL mass as our normalization factor. Unnatural standards introduced at the start of the protocol (tritridecanoin for TAG, 1,2-diheptadecanoyl-*sn*-glycero-3-phospho-(1'-*rac*-glycerol) for PL) are carried through all steps of the solid phase extraction and FAME preparation, and guarantee quantitative and representative recovery of both TAG and PL fractions. The same guarantee cannot be made if investigators use protein or DNA to normalize TAG mass. We believe PL to be the most robust gauge by which to compare TAG levels across samples, as it has been previously shown that PL is only minutely altered by the same stimulus effecting large mass shifts in TAG levels, *e.g.* extended starvation or increased exercise[34-36]. PL are thought to play a structural role, ensuring membrane fluidity and cellular integrity and signaling roles rather than as energy storage[37-39]. In our hands, the TAG/PL ratio most closely matches what is obtained by fixative-based lipid staining with Nile red, and agrees with that found by other groups[21]. An alternative strategy is used by the Watts laboratory, where the percentage of lipid TAG is calculated versus total lipids[9,22,29] .

The use of non-native types of TAG and PL standard ensures that no native fatty acids will be included in the normalization calculation. The choice of chain length is purely based upon the need of these standards to not interfere with the mass spectra of native fatty acids. We have found that fatty acids of 13:0 and 17:0 serve best to this purpose. It is possible, given the different chemical properties of shorter chain fatty acids, that our unnatural fatty acid standards might not be representative of recovery of all chain-length fatty acids or chains with different saturation indices. Thus it is possible that during SPE or GCMS we might see differences in the efficiency of purification or detection between lipids of different chain lengths. Based upon this and the different ionization of different fatty acids in the GCMS, it is not possible to make an absolute statement about the abundance of any given fatty acid. Therefore, we only compare between samples within a single experiment abundances of any given fatty acid. If one wanted to absolutely quantitate a fatty acid, one manner this could be achieved would be to run a sample prepared as above spiked with a known amount of a stably isotopically labeled ^{13}C version of that or similar fatty acid, so that it could be distinguished based upon mass of the parent ion in the MSD, for example. Given that we are only comparing relative amounts of lipid classes or any given fatty acid, our 13:0 TAG and 17:0 PL standards serve this purpose adequately, at a minimum of cost, to assure adequate and representative recovery of each lipid class.

Until this point, there has been a lack of consensus as to the interpretation of certain results obtained by various methodologies, and to what the prevailing methodologies should be. Overall it should be noted that no one method in isolation is ideally suited to study fat metabolism in *C.*

elegans. However, by using multiple screening and validation modalities, one can achieve confidence in data obtained on lipid regulatory genes. Thus, we intend for our protocol to serve as a benchmark for future work in the field of *C. elegans* fat research.

Disclosures

The authors have no conflicting interests to disclose.

Acknowledgements

We would like to thank Michael Kacergis for technical assistance and Lianfeng Wu for discussions and reading the manuscript. This work was supported by a career development award from the NIH/NIDDK (K08DK087941 to A.A.S.), a NIH/NIDDK training grant (5T32DK007028 to E.C.P.), the Ellison Medical Foundation New Scholar in Aging Award (to A.A.S), and the Charles H. Hood Foundation Child Health Research Award (to A.A.S.).

References

1. Zhang, S.O., Trimble, R., Guo, F., & Mak, H.Y. Lipid droplets as ubiquitous fat storage organelles in *C. elegans. BMC Cell biology.* **11**, 96, doi:10.1186/1471-2121-11-96 (2010).
2. Kaletta, T. & Hengartner, M.O. Finding function in novel targets: *C. elegans* as a model organism. *Nature Reviews. Drug Discovery.* **5**, 387-398, doi:10.1038/nrd2031 (2006).
3. Leung, M.C., *et al. Caenorhabditis elegans*: an emerging model in biomedical and environmental toxicology. *Toxicological Sciences: An Official Journal of the Society of Toxicology.* **106**, 5-28, doi:10.1093/toxsci/kfn121 (2008).
4. Ashrafi, K., *et al.* Genome-wide RNAi analysis of *Caenorhabditis elegans* fat regulatory genes. *Nature.* **421**, 268-272 (2003).
5. Arda, H.E., *et al.* Functional modularity of nuclear hormone receptors in a *Caenorhabditis elegans* metabolic gene regulatory network. *Mol. Syst. Biol.* **6**, 367 (2010).
6. Mak, H.Y., Nelson, L.S., Basson, M., Johnson, C.D., & Ruvkun, G. Polygenic control of *Caenorhabditis elegans* fat storage. *Nature Genetics.* **38**, 363-368 (2006).
7. Wang, M.C., O'Rourke, E.J., & Ruvkun, G. Fat metabolism links germline stem cells and longevity in *C. elegans. Science.* **322**, 957-960 (2008).
8. O'Rourke, E.J., Soukas, A.A., Carr, C.E., & Ruvkun, G. *C. elegans* major fats are stored in vesicles distinct from lysosome-related organelles. *Cell Metab.* **10**, 430-435 (2009).
9. Brooks, K.K., Liang, B., & Watts, J.L. The influence of bacterial diet on fat storage in *C. elegans. PLoS ONE.* **4**, e7545, doi:10.1371/journal.pone.0007545 (2009).
10. Yen, K., *et al.* A comparative study of fat storage quantitation in nematode *Caenorhabditis elegans* using label and label-free methods. *PLoS ONE.* **5**, doi:10.1371/journal.pone.0012810 (2010).
11. Rabbitts, B.M., *et al.* glo-3, a novel *Caenorhabditis elegans* gene, is required for lysosome-related organelle biogenesis. *Genetics.* **180**, 857-871, doi:10.1534/genetics.108.093534 (2008).
12. Kimura, K.D., Tissenbaum, H.A., Liu, Y., & Ruvkun, G. daf-2, an insulin receptor-like gene that regulates longevity and diapause in *Caenorhabditis elegans. Science.* **277**, 942-946 (1997).
13. Soukas, A.A., Kane, E.A., Carr, C.E., Melo, J.A., & Ruvkun, G. Rictor/TORC2 regulates fat metabolism, feeding, growth, and life span in *Caenorhabditis elegans. Genes Dev.* **23**, 496-511, (2009).
14. McKay, R.M., McKay, J.P., Avery, L., & Graff, J.M. C elegans: a model for exploring the genetics of fat storage. *Dev. Cell.* **4**, 131-142 (2003).
15. Klapper, M., *et al.* Fluorescence-based fixative and vital staining of lipid droplets in *Caenorhabditis elegans* reveal fat stores using microscopy and flow cytometry approaches. *J. Lipid Res.* **52**, 1281-1293, doi:10.1194/jlr.D011940 (2011).
16. Hellerer, T., *et al.* Monitoring of lipid storage in *Caenorhabditis elegans* using coherent anti-Stokes Raman scattering (CARS) microscopy. *Proc. Natl. Acad. Sci. U.S.A.* **104**, 14658-14663, doi:10.1073/pnas.0703594104 (2007).
17. Wang, M.C., Min, W., Freudiger, C.W., Ruvkun, G., & Xie, X.S. RNAi screening for fat regulatory genes with SRS microscopy. *Nat. Methods.* **8**, 135-138, doi:10.1038/nmeth.1556 (2011).
18. Fowler, S.D. & Greenspan, P. Application of Nile red, a fluorescent hydrophobic probe, for the detection of neutral lipid deposits in tissue sections: comparison with oil red O. *J. Histochem. Cytochem.* **33**, 833-836 (1985).
19. Greenspan, P., Mayer, E.P., & Fowler, S.D. Nile red: a selective fluorescent stain for intracellular lipid droplets. *J. Cell Biol.* **100**, 965-973 (1985).
20. Hope, I.L. Oxford University Press, New York, (1999).
21. Perez, C.L. & Van Gilst, M.R. A 13C isotope labeling strategy reveals the influence of insulin signaling on lipogenesis in *C. elegans. Cell Metab.* **8**, 266-274 (2008).
22. Watts, J.L. & Browse, J. Dietary manipulation implicates lipid signaling in the regulation of germ cell maintenance in *C. elegans. Developmental Biology.* **292**, 381-392, doi:10.1016/j.ydbio.2006.01.013 (2006).
23. Wang, T.J., *et al.* Metabolite profiles and the risk of developing diabetes. *Nature medicine.* **17**, 448-453, doi:10.1038/nm.2307 (2011).
24. Rhee, E.P., *et al.* Lipid profiling identifies a triacylglycerol signature of insulin resistance and improves diabetes prediction in humans. *The Journal of Clinical Investigation.* **121**, 1402-1411, doi:10.1172/JCI44442 (2011).
25. Lewis, G.D., *et al.* Metabolic signatures of exercise in human plasma. *Science translational medicine.* **2**, 33ra37, doi:10.1126/scitranslmed.3001006 (2010).
26. Rhee, E.P., *et al.* Metabolite profiling identifies markers of uremia. *Journal of the American Society of Nephrology : JASN.* **21**, 1041-1051, doi:10.1681/ASN.2009111132 (2010).
27. Gerdt, S., Lochnit, G., Dennis, R.D., & Geyer, R. Isolation and structural analysis of three neutral glycosphingolipids from a mixed population of *Caenorhabditis elegans* (Nematoda:Rhabditida). *Glycobiology.* **7**, 265-275 (1997).
28. Christie, W.W. *Advances in Lipid Methodology - Two.*, Oily Press, 69-111 (1993).

29. Watts, J.L. & Browse, J. Genetic dissection of polyunsaturated fatty acid synthesis in *Caenorhabditis elegans. Proc. Natl. Acad. Sci. U.S.A.* **99**, 5854-5859 (2002).
30. Wahlby, C., *et al.* An image analysis toolbox for high-throughput *C. elegans* assays. *Nat. Methods*. doi:10.1038/nmeth.1984 (2012).
31. Fowler, S.D., Brown, W.J., Warfel, J., & Greenspan, P. Use of nile red for the rapid *in situ* quantitation of lipids on thin-layer chromatograms. *J. Lipid Res.* **28**, 1225-1232 (1987).
32. Squiban, B., Belougne, J., Ewbank, J., & Zugasti, O. Quantitative and Automated High-throughput Genome-wide RNAi Screens in *C. elegans. J. Vis. Exp.* (60), e3448, doi:10.3791/3448 (2012).
33. Leung, C.K., Deonarine, A., Strange, K., & Choe, K.P. High-throughput Screening and Biosensing with Fluorescent C. elegans Strains. *J. Vis. Exp.* (51), e2745, doi:10.3791/2745 (2011).
34. Comizio, R., *et al.* Total body lipid and triglyceride response to energy deficit: relevance to body composition models. *The American journal of physiology.* **274**, E860-866 (1998).
35. Lee, R.F., Paffenhofer, G.A., Nevenzel, J.C., & Benson, A.A. The metabolism of wax ters and other lipids by the marine copepod, *Calanus helgolandicus. J. Lipid Res.* **11**, 237-240 (1970).
36. Lee, S.S., *et al.* Requirement of PPARalpha in maintaining phospholipid and triacylglycerol homeostasis during energy deprivation. *J. Lipid Res.* **45**, 2025-2037, doi:10.1194/jlr.M400078-JLR200 (2004).
37. Singer, S.J. A fluid lipid-globular protein mosaic model of membrane structure. *Annals of the New York Academy of Sciences.* **195**, 16-23 (1972).
38. Singer, S.J. & Nicolson, G.L. The fluid mosaic model of the structure of cell membranes. *Science.* **175**, 720-731 (1972).
39. Turkish, A.R. & Sturley, S.L. The genetics of neutral lipid biosynthesis: an evolutionary perspective. *American Journal of Physiology. Endocrinology and Metabolism.* **297**, E19-27, doi:10.1152/ajpendo.90898.2008 (2009).